Combination of the artificial neural network and advection-dispersion equation for modeling of methylene blue dye removal from aqueous solution using olive stones as reactive bed

Ziad T. Abd Ali

Department of Environmental Engineering, College of Engineering, University of Baghdad, Iraq, Tel. +9647903433954;
email: z.teach2000@yahoo.com

ABSTRACT

In the present investigation, the propensity of olive stones (OS) to be utilized in the removal of methylene blue dye (MBD) from polluted water was analyzed. The three-layer artificial neural network (ANN) model has been used as an alternative method in fixing the relationship describing the sorption process accurately and matching with the experimental results. Therefore, 137 batch experiments were performed for characterizing the equilibrium sorption properties. Applying the ANN model proved that the contact time was the most influential parameter. Subsequently, the transport of methylene blue dye through the OS bed was described by integrating the ANN model with the advection–dispersion equation which describes the transport of contaminant in the porous medium resulting in a good agreement between expected and measured results with a correlation coefficient (R) greater than 0.9789.

Keywords: Biosorption; Olive stones; Methylene blue dye; Artificial neural network; Transport

1. Introduction

All living organisms need water for survival. Pollution of freshwater systems is a subject of concern. Dyes are important pollutants and can be recognized by human eyes. The industrial usage of dyes is as a coloring agent such as leather, plastic, cosmetic, textiles, food, paper, etc. Wastewater discharge from the industries to the resources of water causes problems due to the dyes' worse nature and toxic effect. Water pollution with dyes is harmful because of its toxicity and carcinogenicity [1]. Dyes also inhibit light penetration causing reduction of activities of photosynthetic waterways and disturbing the equilibrium. So, the challenging task is to remove the dyes from the water before discharge. The commonly used dyes are methylene blue dye (MBD) in the coloring of silk, cotton and wool [2]. Using the biosorbents, mostly when employing agricultural by-products and bio waste, makes biosorption valuable and less expensive process [3]. Therefore, the topic of using olive stone as an adsorbent for the removal of dyes has been dealt with by many researchers [4–6], but this study will deal with this material in another perspective. One of the important and interesting topics is the modeling of the process of sorption to predict the partitioning of the pollutants between the solid and aqueous phases and then applying it for assessment of the transporting and fate of the pollutants in the environment. Sorption isotherm models such as Langmuir, Freundlich, Elovich, Temkin, and others are applied frequently for explanation of the equilibrium relationship between the concentrations of the sorbate in the aqueous phase on the one hand and in the solid phase on the other at a specified temperature [7]. In some cases these models do not describe the process of sorption precisely because of their mismatch with the experimental results; therefore,

there is a necessity to use more illustrative models that can distinguish the sorption process [8]. One of the main goal in this study is to find a new way to create a mathematical equation describing the sorption equilibrium relationship and be an alternative to the common isotherm models especially when these models do not match well with the experimental data. Creating these relationships is very beneficial for designing the treatment units, modeling, and many other scientific applications. The advection–dispersion equation was used in this study as one of the scientific applications that need creating this kind of mathematical relationship that has a great match with experimental data to represent accurately the transfer of pollutants in the porous medium. In this consideration, the artificial neural network (ANN) model has got a great interest as an alternative method in fixing a relationship describing the sorption process accurately and matching with the experimental results. Based on the mentioned above, the current study aims to look into the potential application of olive stone biosorbent as a cost-effective material (i) for the removal of MBD from the simulated wastewater, (ii) for illustrating the equilibrium isotherm MBD removal from aqueous media using the ANN model as an alternative to common isotherm models such as Langmuir and Freundlich, and (iii) for characterizing the MBD transport along the reactive bed using the explicit finite difference method (FDM) by integrating the output of the ANN model with a well-known equation that describes the transport of contaminant in the porous medium called "advection-dispersion equation".

2. Experimental work

2.1. Materials

First, the olive stones (OS) were crushed and the 1.2–0.7 mm fraction, obtained after crushing, was selected for the biosorption experiments without any pre-treatment. Subsequently, OS was washed with boiled water, repetitively, with the final washing being done with distilled water to remove any adhering dirt, followed by the drying process carried out at 110°C for 24 h [6]. A few properties, such as porosity, $n = 0.46$, hydraulic conductivity, $K = 8.8$ cm/min, and bulk density, $\rho_b = 0.577$ g/cm^3 of the washed and dried olive stones, were measured at the "Oil Research and Development Center". The methylene blue dye (MBD; $C_{16}H_{18}ClN_3S$) supplied by Loba Chemie (India) was used as an adsorbate without any prior purification. Further, by dissolving 1.0 g of the MBD in 1.0 L of distilled water, the stock dye solution (1,000 mg/L) was prepared, followed by the preparation of the experimental dye solution of desired concentration by diluting the stock solution with a suitable volume of distilled water.

2.2. Batch experiments

The batch experiments were carried out using a series of 250-mL flasks, where 100 mL of MBD solution with an initial concentration of 50 mg/L, was poured into each flask, followed by subsequent addition of about 0.5 g/100 mL of the adsorbent (OS) into these flasks. Mixing of the contents in the flask was carried out by stirring in a high-speed orbital

shaker at 200 rpm for 80 min. Further, the adsorbent was separated by withdrawing a fixed volume (20 mL) of the solution from each flask and was filtered. The residual concentration of MBD, after filtration, was determined using a UV–visible spectrophotometer at a pre-optimised λ_{max} of 665 nm [9]. The kinetic studies were performed at (i) various pH (2.5, 3.5, 4.5, 5.5, 6.5, and 7.5), (ii) different MBD concentration (30, 40, 50, 60, and 70 mg/L), (iii) several adsorbent dosage (0.1, 0.2, 0.3, 0.4, 0.5, 0.6, 0.7, and 0.8 g/100 mL), and (iv) varying agitation speed (50, 100, 150, 200, and 250 rpm). Further, to adjust the pH of the aqueous solution, 0.1 M HCl and 0.1 M NaOH were added, as per requirement. Eventually, the percentage of MBD removal, the output parameter of the ANN model, was estimated as a measure of sorption efficiency of OS. The efficiency of sorption (%) was estimated using Eq. (1):

$$R = \frac{(C_0 - C_e)}{C_0} \times 100 \tag{1}$$

where C_0 and C_e are the initial and equilibrium MBD concentrations (mg/L), respectively. R is the removal efficiency (%). The adsorption capacity of OS at equilibrium, q_e (mg/g), was calculated through Eq. (2):

$$q_e = \frac{V(C_0 - C_e)}{m} \tag{2}$$

where V is the volume of MBD solution (L), and m is the amount of the OS (g).

2.3. Characterization of OS

2.3.1. Scanning electron microscopy

The scanning electron microscopy (SEM) analysis is used for the surface (topography) studies of OS; it is very effective in clarifying all the changes that occur on the surface before and after the accumulation of pollutants. This test was performed using SEM (Inspect S50 Model, FEI/Netherlands).

2.3.2. Fourier-transform infrared

Fourier transfer infrared spectroscopy (FTIR) analysis was carried out to characterize the presence of functional groups on the surface of the OS. Therefore, the OS before and after MBD uptake were examined using Shimadzu FTIR, 8000 series spectrophotometer, Japan.

2.4. Isotherm models

Two isotherm models were used in this study. A summary of these models was presented as cited by Sulaymon et al. [10]:

Freundlich model: is quantified by:

$$q_e = K_f (C_e)^{\frac{1}{n}} \tag{3}$$

where K_f is the Freundlich sorption coefficient and n is an empirical coefficient indicative of the intensity of the adsorption.

Langmuir model: assumes uniform energies of adsorption onto the surface and no transmigration of adsorbate in the plane of the surface. It can be written as follows:

$$q_e = \frac{q_m b C_e}{\left(1 + b C_e\right)} \tag{4}$$

where q_m is the maximum adsorption capacity (mg/g) and b is the constant related to the free energy of adsorption (L/mg).

2.5. Artificial neural networks model

Essentially, the basic working principle of ANNs, also known as "biologically motivated neuron model" is derived from the biological neurons. Typically, a neural network comprises of elementary units called a neuron or node, connected to each other via edges. For computing, the output of these neurons or "neuron impulse" the sum of the input signals from the proceeding neuron undergoes weighted adjustments at the edges, followed by subsequent alteration by the transfer function. Further, with the aim of accomplishing the learning capability of a neuron, the weighting adjustments were carried out by maintaining the congruity with the chosen algorithm. This overall complete process is generally iterative for the ANN. Upon viewing the basic ANN architecture, one can find three types of layers, (a) input, (b) hidden, and (c) output, with the number of neurons in the input and output layer being dependent on the number of input and output parameters, respectively. On the other hand, the determination of the number of neuron in a hidden layer is highly decisive. However, no definite formula exists for its selection [11]. With the aim of correlating the efficiency of the sorption method to remove MBD from the aqueous solution, the ANN model was developed, with Levenberg–Marquardt back propagation (LMA) training algorithm, which was calculated using MATLAB version 7.9 (R2009b). Generally, the number of layers, number of nodes in each layer, and the nature of the transfer functions in an ANN define its topology. Perhaps, the optimization of the ANN topology, the most crucial stage in the development of the model, can be accomplished by dividing the experimental data into three sections; (i) training, (ii) validation, and (iii) test subsets. For this purpose, 83, 27, and 27 samples were employed for training, validation, and test subsets, respectively. Further, the loading of the experimental information into the workspace, for each subset, was carried out in a random manner. Additionally, the neural network utilizes the biggest set, that is, the training data, for assimilating the pattern present in the data by updating the network weights. On the other hand, the testing data were exploited, for evaluating the quality of the network. Eventually, the final check on the achievement and generalization ability of the trained network was executed, by using the validation data.

2.6. Column experiments

In the current study, perspex column having dimensions of 25 cm (height) and 5.0 cm (diameter), and being equipped with three sampling ports made of stainless steel fittings blocked at a distance of 5.0 cm (port 1), 10.0 cm (port

2), and 20.0 cm (port 3) from the bottom of the column, was employed (schematically shown in Fig. 1). Further, a constant head elevated tank was utilized for directing the influent solution in upward flow, with a flow rate of 40 mL/min being determined periodically by the volume of water collected during a period of time. Fundamentally, the upward flow will push the air in front of it and thereby will aid in preventing the occurrence of entrapped air. The column was loaded, with OS in the alignment clarified in Fig. 1, with the elution being carried out at ambient temperature (25°C). Additionally, the concentrations of MBD in the water samples withdrawn from ports 1, 2, and 3 were monitored within time periods ranging from 12 to 120 h. Primarily, the properties (such as compressibility, homogeneity, and porosity) of the reactive material packed in the column were considered constant with the time. Moreover, all fittings and appurtenances for the used column were composed of inert material.

3. Results and discussion

3.1. Development and optimization of the ANN model

In the current investigation, the tangent sigmoid transfer function (tansig) and a linear transfer function (purelin) were used at hidden layer and at the output layer, respectively. Further, (i) contact time (min), (ii) initial pH, (iii) agitation speed (rpm), (iv) initial MB concentration (mg/L), and (v) dosage of OS (g/100 mL) were the input variables to the feed-forward neural network. While the removal efficiency (%), the experimental response, was designated as the output variable. The minimum value of the mean square error (MSE) of the training and prediction set served as a basis for determining the optimal architecture of the ANN model and variations in the parameter. Moreover, in the network optimization, two neurons in the hidden layer were utilized
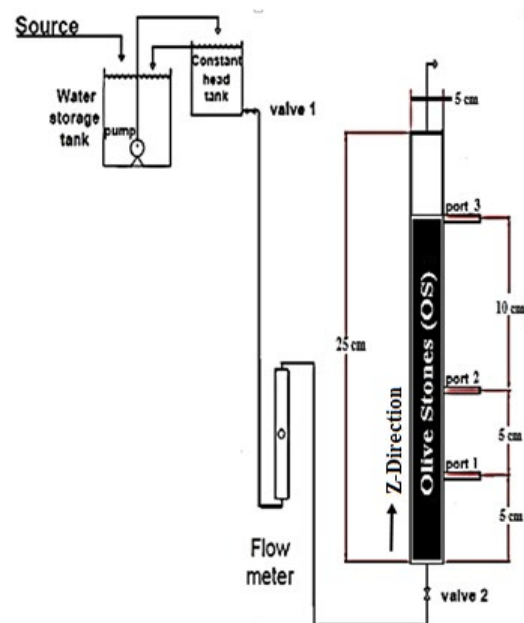

Fig. 1. Schematic diagram of the laboratory-scale column.

as an initial guess. However, accretion in the number of neurons resulted in several local minimum values from the network, in addition to, attainment of different MSE values for the training set. Fig. 2 evidently illustrates that the highest value of MSE (=0.009) of the network was obtained, with 2.0 hidden neurons. While an increment in the number of neurons from 2.0 to 4.0 causes a significant lowering in the MSE value from 0.009 to 0.0012, which further decreases and reaches its minimum value of 0.00025, with 10.0 hidden neurons. These observations lead to the selection of the neural network containing 10.0 hidden neurons, as the best case. However, a further increment in the number of neurons from 10.0 to 15.0 resulted in an increase in the MSE value. The increment was attributable to the features of the MSE performance index and the input vector used in the present study. Further, the inception of the increase in the differences between training error and validation error led to the discontinuation of the training after 183 epochs for the LMA. Fig. 3 depicts the training, validation, and test means square errors
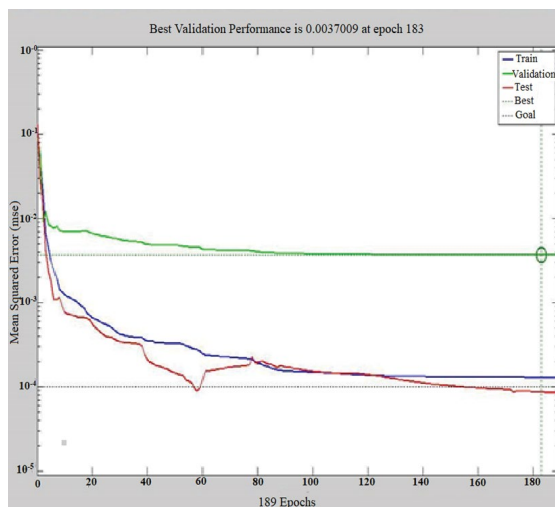
for the LMA. Ultimately, for prediction of MBD removal from aqueous solution via the biosorption method, the optimal ANN structure was found to be 5:10:1 (Fig. 4). On the other hand, Fig. 5 establishes the better regression for training, validation, and testing for the Levenberg–Marquardt algorithm, where one can clearly witness the correlation coefficient for training, validation, testing, and all data to be 0.9987, 0.95532, 0.99933, and 0.99097, respectively.

3.2. Influence of batch operating parameters

3.2.1. Effect of contact time and initial pH of solution

Upon analyzing the results obtained from the biosorption of MBD on the OS, a contact time of 70 min was established as an adequate period for achieving equilibrium, because a further increase in contact time did not lead to any significant changes in the sorption (Fig. 6). The observation gives a clear indication that the removal efficiency, in the beginning, increased rapidly and subsequently became constant until the sorption process reaches the equilibrium state. The abundance of vacant active sites on the surface of the OS, possibly explains the rapid increase at the commencement. On the contrary, the diffusion of MBD into the pores of the adsorbent, since the external sites are being completely occupied, is mainly responsible for the slow increase at the later stage [9].

The analysis also unveils the vital contribution of solution pH, in the chemistry of both the OS biomass and MBD molecules, in addition to, its significant repercussions on electrostatic charges, being imparted by ionized dye molecules [6]. Fig. 6 clearly depicts the dependency of the removal of MBD from aqueous solution on the pH of the solution. It mainly occurs due to the presence of various functional groups such as hydroxyl, carbonyl, and an amine group, being distributed on the surface of OS, which acts as a binding site and generally gets affected by the pH of the solution [12]. With an increase in the pH of the MBD solution, the amount
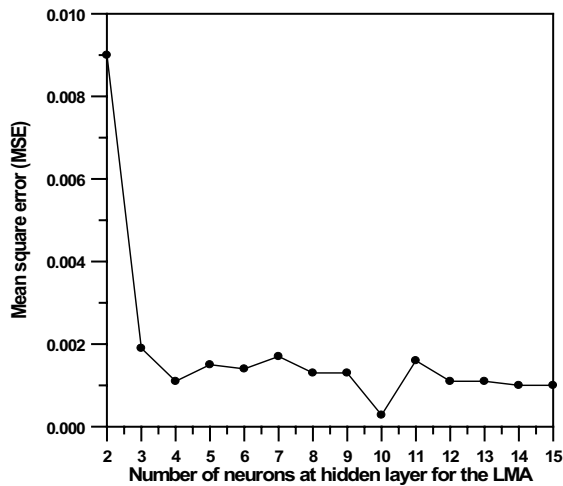

Fig. 2. Dependence between MSE and number of neurons at hidden layer for the LMA.

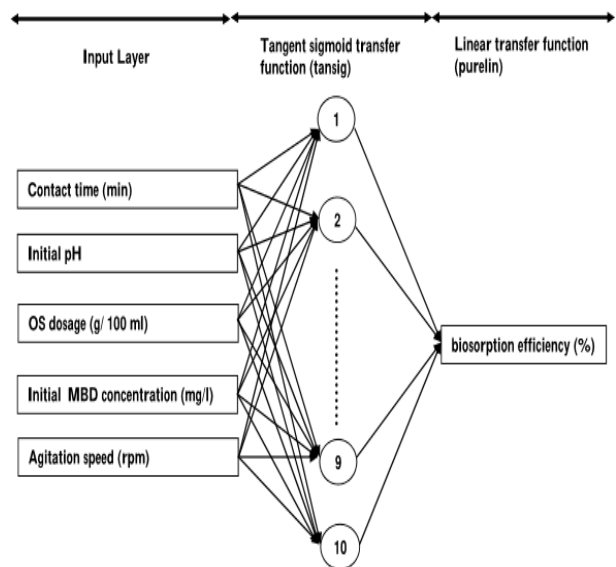Fig. 3. Training, validation, and test mean square errors for the Levenberg–Marquardt algorithm.

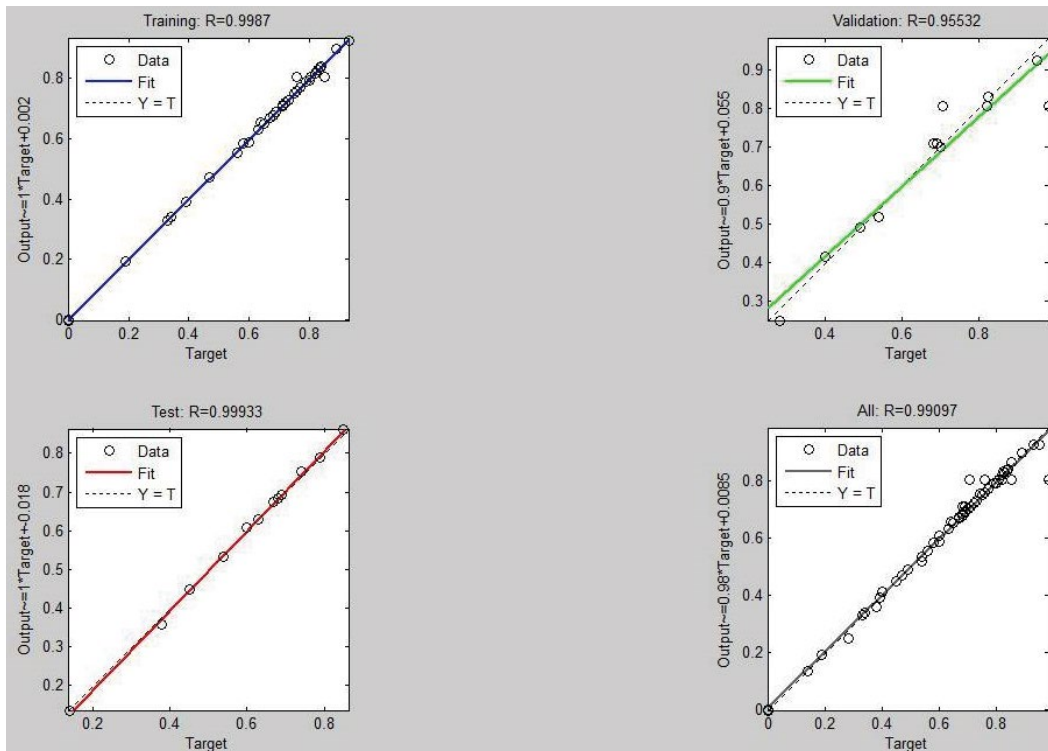Fig. 4. Optimal architecture of ANN.

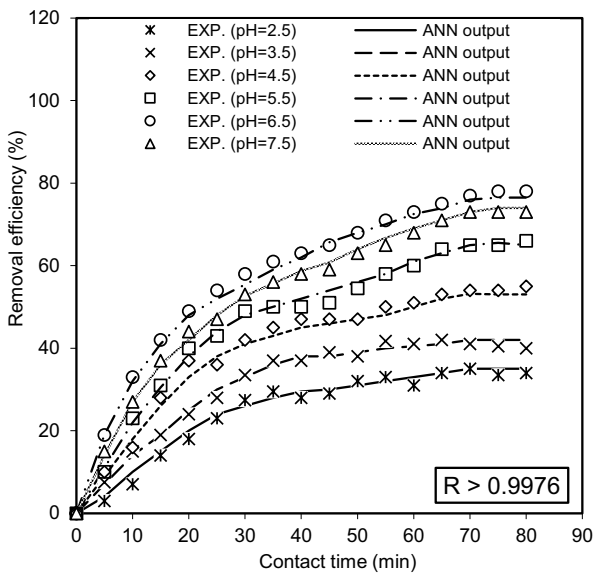Fig. 5. Training, validation, and testing regression for the Levenberg–Marquardt algorithm.

Fig. 6. Agreement between ANN outputs and experimental data as a function of pH (C_0 = 50 mg/L, OS dosage = 0.5 g/100 mL, agitation speed = 200 rpm).

of sorbed MBD increases, with the maximum removal efficiency of MBD reaching a value of 76%, at pH 6.5. Previously, the point of zero charges of the olive stone biomass has been estimated as 5.17 [13]. Therefore, the electrostatic interaction between the negatively charged surfaces of the biosorbent and the cationic dye, at pH > pH_{PZC}, can entirely explicate the above-observed trend [14]. Nevertheless, for examining the

effects of other working parameters on the efficiency of MBD removal, in other batch experiments, pH 6.5 was found to be the optimal initial pH. Fig. 6 also displays the agreement between the ANN model predictions and the experimental data as a function of the initial pH of the solution. The figure manifests a good agreement between the obtained results from the proposed ANN model and the experimental data with a correlation coefficient greater than 0.9976.

3.2.2. Effect of agitation speed

Fig. 7 reveals that with an increase in the agitation speed from 50 to 250 rpm, the removal efficiency increases gradually, due to the increased diffusion rate of contaminant (MBD) towards the surface of the reactive media (OS). As a result, the contact between the contaminant and the binding sites can be accomplished in an adequate manner [15]. Additionally, from Fig. 7 one can also conclude that for the experimental data, the ANN model shows a good prediction, with a correlation coefficient of 0.9975.

3.2.3. Effect of initial MBD concentration

As indicated by Fig. 8, the removal efficiency of MBD undergoes a reduction, with an increase in the initial concentration from 30 to 70 mg/L. These observations can be attributed, to the involvement of energetically less favorable sites with increasing concentrations in the aqueous solution [16]. The figure also reveals a good prediction of the experimental data by the ANN model, with a correlation coefficient of 0.99.
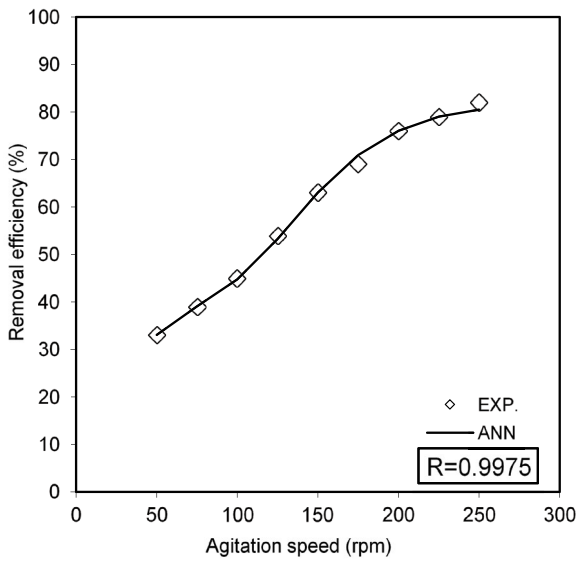
Fig. 7. Agreement between ANN outputs and experimental data as a function of agitation speed (C_0 = 50 mg/L, OS dosage = 0.5 g/100 mL, t = 70 min, pH = 6.5).
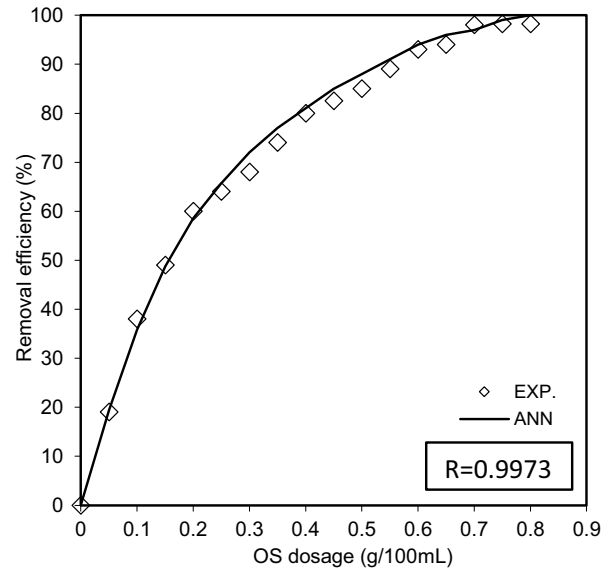

Fig. 9. Agreement between ANN outputs and experimental data as a function of adsorbent dosage (C_0 = 30 mg/L, t = 70 min, pH = 6.5, agitation speed = 250 rpm).
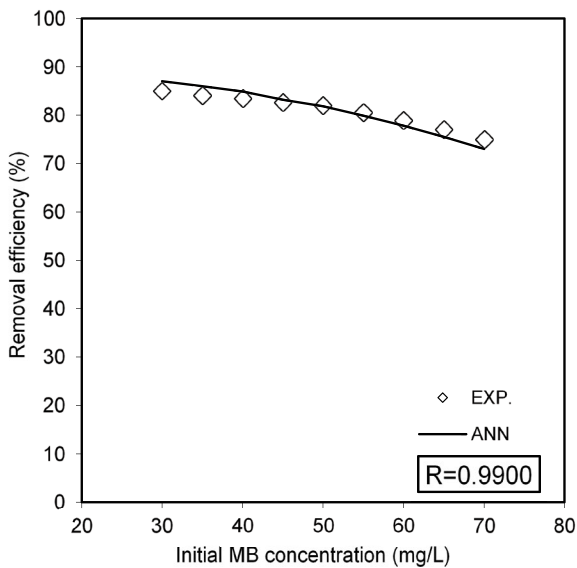

Fig. 8. Agreement between ANN outputs and experimental data as a function of initial MBD concentration (OS dosage = 0.5 g/100 mL, t = 70 min, pH = 6.5, agitation speed = 250 rpm).

3.2.4. Effect of OS dosage

From Fig. 9, it is evident that for a fixed initial MBD concentration of 30 mg/L, the removal efficiency of MBD onto OS gets improved with increasing adsorbent dosage from 0.05 to 0.8 g, with an observation of no significant changes further. The increase in the removal efficiency, as expected, occurs due to the greater availability of sorption sites, with the addition of a higher dosage of adsorbent in the solution [17]. Fig. 9 also compares the ANN model predictions with the experimental data as a function of adsorbent dosage,

thereby indicating a satisfactory prediction of the trend of the experimental data by the ANN model, with a correlation coefficient of 0.9973.

3.3. Biosorption of MBD

The ANN model also illustrated the biosorption data as a function of equilibrium MBD concentration (C_e) and the corresponding equilibrium sorption capacity (q_e). To evaluate the ANN model and the extent of its representation of the sorption data accurately, two isotherm models (Freundlich and Langmuir) were used. The constants of these models were calculated by non-linear estimation using "STATISTICA 8" software as illustrated in Table 1. Fig. 10 shows the experimental results and compares their representation using Freundlich, Langmuir, and ANN models. It explains that the results of the ANN model have the highest match (R = 0.9952) with the experimental data compared with the results of isotherm models ($R \leq 0.8798$), with the calculated maximum sorption capacity found to be 10.2 mg/g. Based on these results, the ANN model was fitted with a polynomial relationship (Eq. (5)) using Microsoft Excel 2007 software as illustrated in Fig. 10. This relationship represents a flexible framework having the potential to be applied for describing the outputs of the ANN model as the most accurate representation of the sorption data compared with isotherm models [$q_e = f(C)$]:

$$q_e = -\alpha_1 C^6 + \alpha_2 C^5 - \alpha_3 C^4 + \alpha_4 C^3 - \alpha_5 C^2 + \alpha_6 C + \alpha_7 \ (R = 0.9865)$$

(5)

This equation in combination with the advection–dispersion equation (Eq. (7)) forms an integrated model, which is useful in predicting the sorption effects on the performance of the OS reactive bed (packed column).

3.4. Results of OS characterization

3.4.1. SEM analysis

Fig. 11 shows the topography of the OS before and after sorption of MBD, as depicted in this figure the OS surface before sorption is irregular and heterogeneous with noticeable pores and fiber-like structures, these characteristics will lead to an increase in the uptake capacity of MBD solution. After the sorption of MBD, the surface of the OS is smoother signifying that the MBD has adhered densely and uniformly on the OS surface.

3.4.2. FTIR analysis

Identification of the characteristic functional groups, responsible for MBD binding, on the surface of the OS, primarily can be done by using the FTIR analysis [18]. Upon analysis, the observed displacement in the infrared frequencies corroborates the functional groups such as alcohols, carboxylic acids, amines, esters, aromatic, and alkyl halides, to be responsible for the sorption of MBD onto OS as shown in Fig. 12 and Table 2. Accordingly, the adsorption process may be the mechanism involved in controlling the sorption of MBD onto OS supported by the existence of the functional groups which are defined before.

3.5. Sensitivity analysis

Depending on the neural net weight matrix and Garson equation (1991) illustrated as follows [19]:

$$I_j = \frac{\sum_{m=1}^{m=Nh}\left(\left(\dfrac{\left|W_{jm}^{ih}\right|}{\sum_{k=1}^{Ni}\left|W_{km}^{ih}\right|}\right) \times \left|W_{mn}^{ho}\right|\right)}{\sum_{k=1}^{k=Ni}\left\{\sum_{m=1}^{m=Nh}\left(\dfrac{W_{km}^{ih}}{\sum_{k=1}^{Ni}\left|W_{km}^{ih}\right|}\right) \times \left|W_{mn}^{ho}\right|\right\}} \tag{6}$$

where I_j is the relative importance of the jth input variable on the output variable, Ni and Nh are the numbers of input and hidden neurons, respectively, $W's$ are connection weights, the superscripts i, h, and o refer to input, hidden, and output layers, respectively, and subscripts k, m, and n refer to input, hidden, and output neurons, respectively. The sensitivity

Table 1
Parameters of isotherm models for sorption of MBD onto OS

Isotherm model	Parameter
Freundlich	K_f (mg/g)(L/mg)$^{1/n}$ 3.9805
	n 3.4392
	R 0.8798
Langmuir	q_m (mg/g) 8.5002
	b (L/mg) 0.9576
	R 0.7792

Fitted Polynomial Eq. for ANN Model
$Y = -0.0002X^6 + 0.0083X^5 - 0.1496X^4 + 1.2549X^3 - 4.9183X^2 + 8.2699X + 0.6057$
$(R = 0.9865)$

◇ Experimental
------ Freundlich Model (R=0.8798)
— — Langmuir Model (R=0.7792)
—— ANN. Model (R=0.9952)

Fig. 10. Comparison of the experimental results with the q_e values obtained by different models.
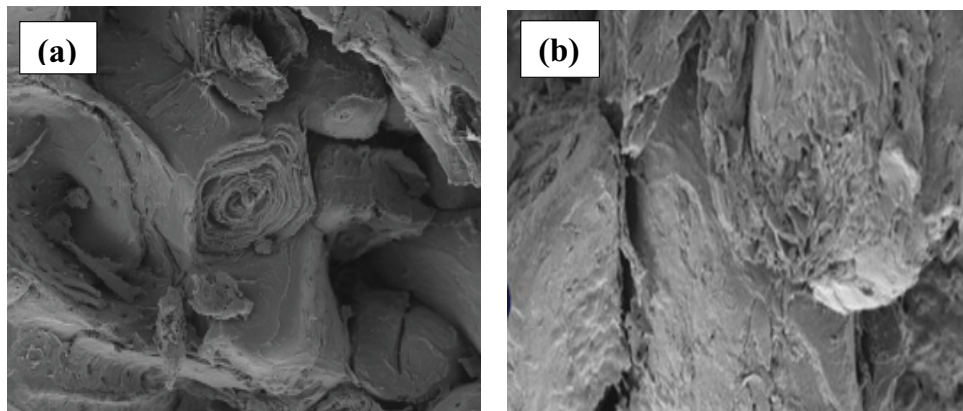

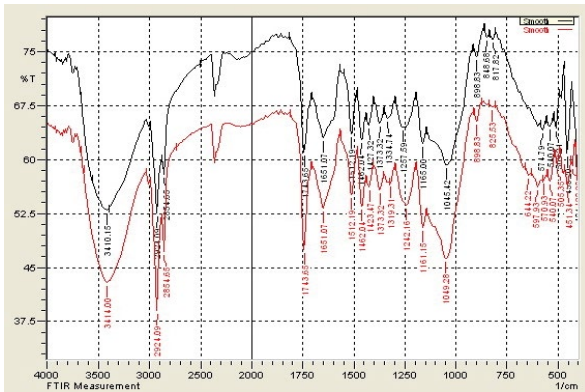Fig. 11. SEM images of OS (a) before and (b) after sorption of MBD.

Fig. 12. IR spectrum of OS before and after sorption of MBD.

Table 2
Functional groups responsible for MBD sorption onto OS

Functional group	Type of bond	Wave No. (cm^{-1}) before MBD loading	Wave No. (cm^{-1}) after MBD loading
Alcohols	N–H$_2$ stretch	3,410.15	3,414.00
Carboxylic acids	O–H bend	1,427.32	1,423.47
Amines	C–N stretch	1,334.74	1,319.31
Esters	C–C(O)–C stretch	1,257.59	1,242.16
Alcohols	O–H stretch	1,045.42	1,049.28
Aromatic	C–H bend	817.82	825.53
Alkyl halides	–C–Br stretch	574.79	597.93

analysis was carried out for stipulating the relative importance of the input variables, demonstrated in the following way: among all the parameters analyzed, the contact time with a relative importance of 28%, exerted its influence to a larger extent in the biosorption process of MBD onto the OS and thereby appears to be the most influential parameter. Further, the impact imparted by other parameters follows the sequence of initial pH of the solution, initial concentration, agitation speed, OS dosage, with the relative importance values to be 24%, 21%, 17%, and 10%, respectively. However, depending upon the experimental ranges, the detection of the effect of each variable and influential variable was envisioned during the fitting of the ANN model [20].

3.6. Transport of MBD through OS packed column

The combination of the advection–dispersion equation (Eq. (7)) and outputs of ANN (Eq. (5)) represents the integrated model developed in the present study for describing the MBD transport in a porous medium (OS).

$$D_z \frac{\partial^2 C_{MBD}}{\partial z^2} - V_z \frac{\partial C_{MBD}}{\partial z} = \frac{\partial C_{MBD}}{\partial t} + \frac{\rho_b}{n} \frac{\partial q}{\partial t} \tag{7}$$

where D_z is the dispersion coefficient in the direction z (cm /s), V_z is the velocity of flow (cm/s), C_{MBD} represents the

MBD concentration in the aqueous solution (mg/L), q is the MBD concentration adsorbed on the solid phase, OS, (mg/g), n is the porosity of the medium, and ρ_b is the dry sorbing material bulk density (g/cm^3). The biosorption of MBD on the OS was described, in the present study, by substituting q in the second term on the right-hand side of Eq. (7) by Eq. (5) which represents an alternative to the isotherm models under isotherm conditions. Further, for ascertaining the spatial and temporal distribution of the contaminant, explicit FDM was used as follows:

$$C_i^{n+1} = C_i^n + \left(\frac{(\Delta t)(D_z)}{R} \right) \left(\frac{C_{i-1}^n - 2C_i^n + C_{i+1}^n}{(\Delta z)^2} \right) - \left(\frac{(\Delta t)(V_z)}{R} \right) \left(\frac{C_i^n - C_{i-1}^n}{\Delta z} \right) \tag{8}$$

where the superscript $n + 1$ and n are the next and present time step, respectively; $\Delta t = t^{n+1} - t^n$ is the time step size, and i, $i + 1$, $i - 1$ are the grid identification, and R is the retardation factor (Eq. (9)).

$$R = 1 + \frac{\rho b}{n} \frac{\partial q}{\partial C} \tag{9}$$

The initial and boundary conditions describing the status of continuous experiments were used in the following way: (i) the concentrations of the initial liquid and solid contaminants were presumed to be zero through the flow domain. (ii) The boundary conditions were considered, at the bottom of the column ($z = 0$), the concentration of MBD is equal to 30 mg/L, and at the top of the column ($z = 20$ cm), the flux is advective (InlineEqn(1)). (iii) The discretized algebraic equation in combination with ANN was formulated, followed by the subsequent development of the computer program, written in MATLAB version 7.9 (R2009b), for its implementation.

As a consequence of the biosorption processes, dissolved MBD will travel through the sorbent bed with extremely slow speed in comparison with the feed solution that transports them. In other words, the flow of MBD in the solution gets decelerated, and this deceleration is known as retardation effect [21]. Further, in Fig. 13, breakthrough curves of MBD in the effluent of selected ports 1, 2, and 3 were observed, which in turn serves as evidence of an increase in both the numerical (FDM solution) and experimental (EXP.) normalized concentrations with time. The figure also demonstrated more effective treatment upon augmentation of the thickness of the packed bed. Indeed, this happens due to the increase in the retention time of the pollutant within the bed, with an increase in the thickness of the bed, which in turn results in better sorption process. In the same way, the longevity of the reactive bed, the time required for sustaining the contaminant concentration in the effluent less than the quality limit, increases with an increase in the thickness of the bed. However, with a rise in the travel time of the contaminant, the bed appears to get saturated, which in turn causes a reduction in the contaminant retardation factor, and thereby weakens the functionality of the reactive bed. Apart from the above facts, Fig. 13 also affirms a good prediction, in the case of the
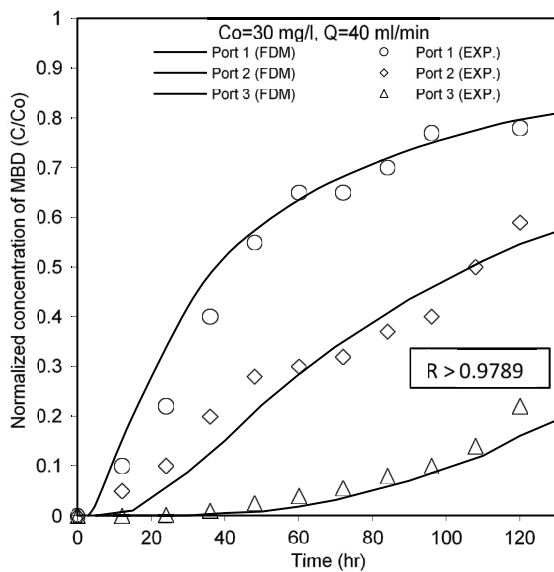
Fig. 13. Breakthrough curves as a result of the MBD transport at selected ports along the column packed with OS reactive bed.

Explicit FDM solution, for the experimental data with a correlation coefficient (*R*) greater than 0.9789. Thus, it demonstrates that the numerical solution procedure provides an illustrative picture of the contaminant distribution throughout the reactive bed. Therefore, the breakthrough curves of a recognized pollutant for two different values of flow rate (10, 20 mL/min) at the port (1, 2), in addition to, the variation of normalized concentrations along the length of the bed can be prognosticated as shown in Fig. 14. This figure shows the vital role of the bed in limiting the propagation of the contaminant plume. Moreover, it looks that increasing the flow rate leads to more propagation of the contaminant front.

4. Conclusions

- From the batch experiments, carried out for removal of MBD from solutions using OS as cost-effective biosorbent, the best-operating conditions were found to be (i) an initial pH of 6.5, (ii) 0.7 g/100 mL of OS dosage, (iii) an initial MBD concentration of 30 mg/L, and (iv) an agitation speed of 250 rpm. Additionally, for achieving the maximum removal efficiency of 98%, with the maximum sorption capacity to be 10.2 mg/g, the contact time of 70 min was found to be appropriate.
- FTIR analysis proved that the alcohols, carboxylic acids, amines, esters, aromatic, and alkyl halides were responsible for the biosorption of MBD onto OS.
- The efficiency of the MBD removal was anticipated to be predicted by a three-layer ANN with a tangent sigmoid transfer function and a linear transfer function at the hidden layer and the output layer, respectively. For this purpose, the optimal number of the neuron, in the case of LMA, was determined to be 10.0 hidden neurons with MSE of 0.00025. The proposed ANN model predicted the experimental data effectively, with a correlation coefficient greater than 0.99 for five operating variables. Remarkably, the sensitivity analysis confirmed
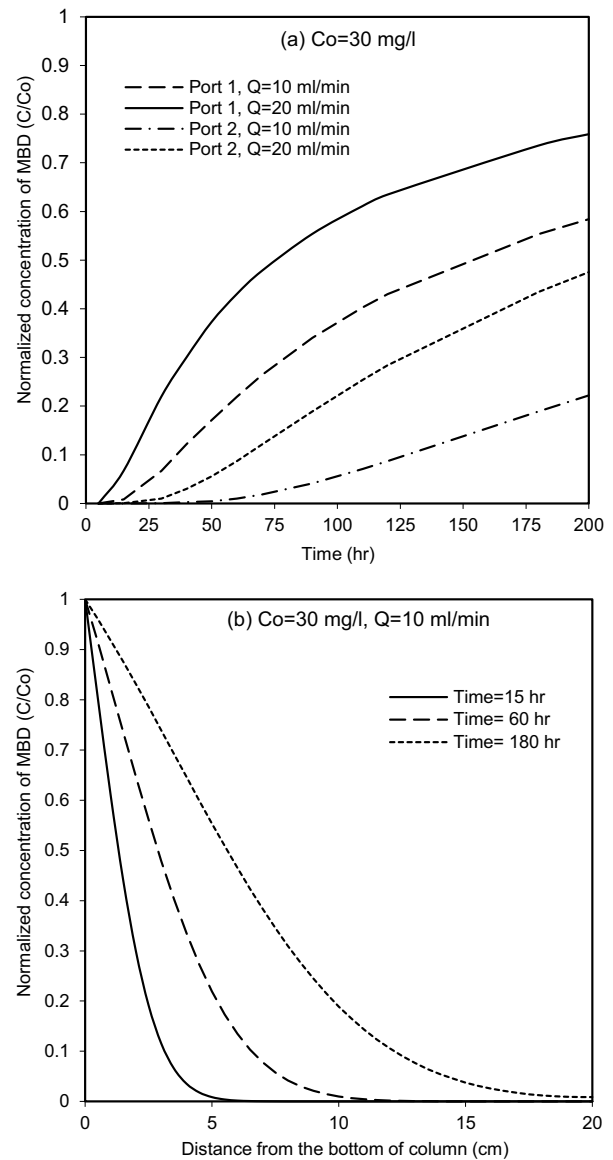

Fig. 14. Predicted variation of MBD normalized concentration (a) temporally and (b) spatially in the column packed with OS reactive bed.

the contact time, with a relative importance of 28%, to be the most pivotal parameter in the removal process followed by initial pH of the solution, initial concentration, agitation speed, and OS dosage.
- Prominently, the ANN outputs as an alternative to the isotherm models in the advection–dispersion equation with using FDM were found to act as an effective and efficient tool for the illustration of the MBD migration through the OS packed column with a correlation coefficient greater than 0.978.

References

[1] K. Vikrant, B.S. Giri, N. Raza, K. Roy, K.-H. Kim, B.N. Rai, R.S. Singh, Recent advancements in bioremediation of dye: Current status and challenges, Bioresour. Technol., 253 (2018) 355–367.

[2] R. Kabbout, S. Taha, Biodecolorization of textile dye effluent by biosorption on fungal biomass materials, Phy. Procedia, 55 (2014) 437–444.

[3] M.-X. Wang, Q.-L. Zhang, S.-J. Yao, A novel biosorbent formed of marine-derived penicillium janthinellum mycelial pellets for removing dyes from dye-containing wastewater, Chem. Eng. J., 259 (2015) 837–844.

[4] S. Dardouri, A. Jedidi, J. Sghaier, Efficient Removal of Methylene Blue from Aqueous Solutions Using Olive Stone and Rye Straw as Abundant Adsorbents, in Recent Advances in Science, Technology & Innovation, 2018, pp. 119–121

[5] S. Dardouri, J. Sghaier, Adsorptive removal of methylene blue from aqueous solution using different agricultural wastes as adsorbents, Korean J. Chem. Eng., 34 (2017) 1037–1043.

[6] A.B. Albadarin, C. Mangwandi, Mechanisms of Alizarin Red S and Methylene blue biosorption onto olive stone by-product: isotherm study in single and binary systems, J. Environ. Manage., 164 (2015) 86–93.

[7] O. Hamdaouia, E. Naffrechoux, Modeling of adsorption isotherms of phenol and chlorophenols onto granular activated carbon Part I. Two-parameter models and equations allowing determination of thermodynamic parameters, J. Hazard. Mater., 147 (2007) 381–394.

[8] Z.B. Bouabidi, M.H. El-Naas, D. Cortes, G. Mc Kay, Steel-making dust as a potential adsorbent for the removal of lead (II) from an aqueous solution, Chem. Eng. J., 334 (2018) 837–844.

[9] S. Shakoor, A. Nasar, Removal of methylene blue dye from artificially contaminated water using citrus limetta peel waste as a very low-cost adsorbent, J. Taiwan Inst. Chem. Eng., 66 (2016) 154–163.

[10] A.H. Sulaymon, A.A.H. Faisal, Z.T. Abd Ali, Performance of granular dead anaerobic sludge as permeable reactive barrier for containment of lead from contaminated groundwater, Desal. Wat. Treat., 56 (2015) 327–337.

[11] Y.A. Mustafa, G.M. Jaid, A.I. Alwared, M. Ebrahim, The use of artificial neural network (ANN) for the prediction and simulation of oil degradation in wastewater by AOP, Environ. Sci. Pollut. Res., 21 (2014) 7530–7537.

[12] G. Blazquez, M. Calero, A. Ronda, G. Tenorio, M.A. Martín-Lara, Study of kinetics in the biosorption of lead onto native and chemically treated olive stone, J. Ind. Eng. Chem., 20 (2014) 2754–2760.

[13] A. Ronda, M.A. Martín-Lara, M. Calero, G. Bla´zquez, Analysis of the kinetics of lead biosorption using native and chemically treated olive tree pruning, Ecol. Eng., 58 (2013) 278–285.

[14] J. Galan, A. Rodríguez, J M. Gomez, S J. Allen, G M. Walker, Reactive dye adsorption onto a novel mesoporous carbon, Chem. Eng. J., 219 (2013) 62–68.

[15] A.A.H. Faisal, Z.T. Abd Ali, Using sewage sludge as permeable reactive barrier for remediation of groundwater contaminated with lead and phenol, Sep. Sci. Technol., 52 (2017) 732–742.

[16] M. Selvarani, P. Prema, Removal of toxic metal hexavalent chromium [Cr (VI)] from aqueous solution using starch – stabilized nanoscale zero valent iron as adsorbent: equilibrium and kinetics, Int. J. Environ. Sci., 2 (2010) 1962–1975.

[17] A.A.H. Faisal, Z.T. Abd Ali, Remediation of groundwater contaminated with the lead–phenol binary system by granular dead anaerobic sludge-permeable reactive barrier, Environ. Technol., 38 (2017) 2534–2542.

[18] J.P. Chen, L. Wang, S.-W. Zou, Determination of lead biosorption properties by experimental and modeling simulation study, Chem. Eng. J., 131 (2007) 209–215.

[19] A. Aleboyeh, M.B. Kasiri, M.E. Olya, H. Aleboyeh, Prediction of azo dye decolorization by UV/H2O2 using artificial neural networks, Dyes Pigm., 77 (2008) 288–294.

[20] Y. Yang, X. Lin, B. Wei, Y. Zhao, J. Wang, Evaluation of adsorption potential of bamboo biochar for metal-complex dye: equilibrium, kinetics and artificial neural network modeling, Int. J. Environ. Sci. Technol., 11 (2014) 1093–1100.

[21] C.W. Fetter, Contaminant hydrogeology, 2nd ed. Prentice-Hall, New Jersey, 1999.